

Photoelectron imaging spectroscopy of $\text{Cu}^-(\text{H}_2\text{O})_{1,2}$ anion complexes

G. Jeffrey Rathbone, Todd Sanford, Django Andrews, W. Carl Lineberger *

JILA and Department of Chemistry and Biochemistry, University of Colorado, Box 440, UCB, Boulder, CO 80309, USA

Received 1 November 2004; in final form 23 November 2004

Available online 15 December 2004

Abstract

We report high resolution photoelectron imaging spectra of Cu^- and $\text{Cu}^-(\text{H}_2\text{O})_n$ ($n = 1, 2$) complexes. With the least bound electron principally localized on the metal, electron photodetachment produces neutral states that are best characterized by the atomic metal state plus a water molecule: $[\text{Cu}(^2\text{S}), \text{H}_2\text{O}]$, $[\text{Cu}(^2\text{D}_{5/2}), \text{H}_2\text{O}]$, and $[\text{Cu}(^2\text{D}_{3/2}), \text{H}_2\text{O}]$. The large Cu^- – H_2O separation gives rise to a remarkably narrow, isolated peak in the photoelectron spectrum, allowing an accurate, direct determination of the anion dissociation energy; when coupled with electronic structure calculations for the neutral, the adiabatic electron affinity is derived.

© 2004 Elsevier B.V. All rights reserved.

1. Introduction

Recent experiments [1] and calculations [2,3] of the structure and rearrangement dynamics of CuH_2O following electron photodetachment from $\text{Cu}^-\text{H}_2\text{O}$ have afforded considerable insight into the ultrafast solvent motions in the evolving complex. The initial configuration of the complex was derived from ab initio calculations and a low resolution (~ 0.25 eV) photoelectron spectrum of $\text{Cu}^-\text{H}_2\text{O}$ obtained by Misaizu et al. [4,5]. In order both to assess the calculations and to obtain more accurate thermochemical information for this complex, we employ a new photoelectron imaging spectrometer to obtain high resolution photoelectron spectra of Cu^- and $\text{Cu}^-(\text{H}_2\text{O})_{1,2}$.

The imaging technique developed by Chandler and Houston [6] has become an invaluable tool for study of gas-phase dynamics [7–9]. When employed in the velocity map imaging mode developed by Eppink and Parker [10], significantly higher resolution photoelectron images can be acquired, while maintaining the 4π collection efficiency of the imaging technique. Recently, Sanov

and coworkers [11–14] and Neumark and coworkers [15–17] have extended this imaging technique to anions, incorporating imaging into a pulsed ion beam photoelectron spectrometer. In the work reported here, we employ pulsed ion source technologies [18] to produce copper–water anion complexes and obtain high resolution photoelectron spectra using velocity map photoelectron imaging.

Qualitative expectations of the structure of the copper–water negative ion complex would orient the hydrogen atoms of water toward the metal anion, with a relatively long bond distance as a result of the expanded $4s$ orbital in the $\text{Cu}^- 3d^{10} 4s^2 ^1\text{S}$ ground state. In the neutral copper–water complex, the oxygen atom should be oriented toward the metal. Photodetachment of one of the $\text{Cu}^- 4s^2$ electrons produces the electronic ground state of the complex at the anion configuration, i.e., with the hydrogen atoms still oriented toward the metal atom. The smaller spatial extent of the $4s$ outer-shell electron orbitals of neutral $\text{Cu } 4s ^2\text{S}$ (compared with the diffuse, doubly occupied $4s^2$ orbital of the $\text{Cu}^- 4s^2 ^1\text{S}$ anion) provides a significant simplification of the photoelectron spectra of the $\text{Cu}^-(\text{H}_2\text{O})_n$ complexes. Electron photodetachment of one of the $\text{Cu}^- 4s^2$ electrons forms the neutral complex at the anion geometry, with such a large copper–water separation that the inter-

* Corresponding author. Fax: +1 303 492 8994.

E-mail address: wcl@jila.colorado.edu (W.C. Lineberger).

actions between Cu $4s^2S$ and water will be relatively weak. On the other hand, detachment of one of the $3d^{10}$ electrons of Cu^- , producing Cu $3d^9 4s^2^2D$, gives rise to a electronically excited neutral complex with an equilibrium copper–oxygen bond length that is comparable to that of the anion. When electron photodetachment produces this state, significantly stronger Cu–H₂O interactions should be present than when the ground state is formed, giving rise to a broadened peak (or, if resolved, a more extended progression) in the photoelectron spectrum. These qualitative pictures are supported by recent elaborate calculations of the anion and neutral complexes [2], as summarized in Fig. 1. Overall, the $Cu^-(H_2O)_n$ photoelectron spectra should resemble the Cu^- photoelectron spectrum [19], shifted to increasingly higher binding energies as the degree of solvation increases.

This Letter briefly describes a new, high-resolution negative ion photoelectron imaging spectrometer, and presents results for Cu^- and $Cu^-(H_2O)_n$ ($n = 1, 2$). From these data electron affinities and binding energies for the complexes are determined.

2. Experimental apparatus

The basic ion beam machine consists of a sputtering ion source coupled with a Wiley–McLaren [20] time-of-flight mass spectrometer with a second, reflectron mass spectrometer to detect the ionic photoproducts,

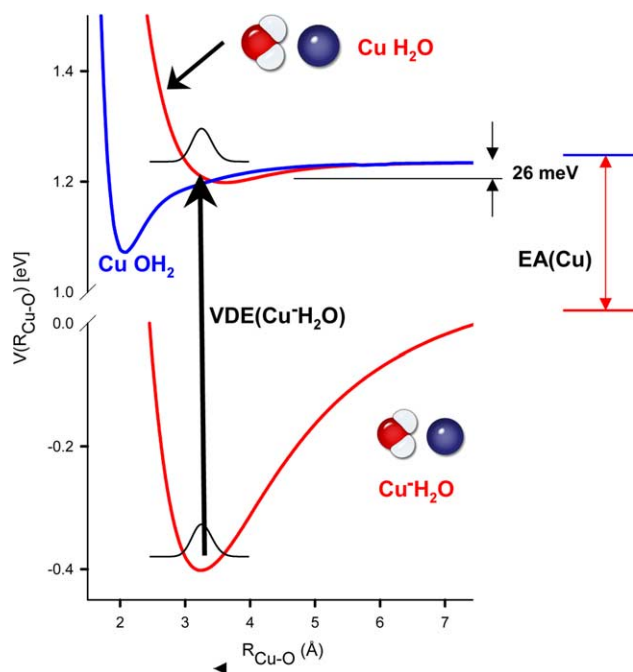


Fig. 1. Potential energy surfaces and structures for C_{2v} $Cu^-(H_2O)$ and $Cu(H_2O)$. The CuH_2O potential with the short bond length corresponds to the water oxygen atom oriented toward the copper atom [2].

as has been described [21,22] in detail. A sputtering ion source produces significant quantities of Cu^- , $Cu^-(H_2O)_{1,2}$ ions, with an estimated molecular ion temperature of 150–300 K [1]. At the spatial focus of the time-of-flight mass spectrometer, the ions are intercepted by tunable radiation produced by a Coherent Infinity Nd:YAG-pumped optical parametric oscillator, with pulse energies variable from hundreds of nanojoules to several millijoules. A newly constructed photoelectron imaging system is located at this spatial focus, extracting photoelectrons perpendicular to the 3 keV ion beam and operated in the velocity map imaging [10,12] mode. After traveling 20 cm in the μ -metal shielded flight tube, the photoelectrons encounter a gated, 40 mm diameter microchannel plate detector, followed by a phosphor screen. A cooled CCD camera (La Vision) obtains photoelectron images in an event counting mode, whereby the centroid of each individual photoelectron event is recorded. The three-dimensional photoelectron velocity and angular distributions are reconstructed from the raw two-dimensional images using the BASEX image reconstruction method developed by Reisler and coworkers [23]. As this photoelectron imaging spectrometer is very similar to that described by Sanov and coworkers [12,14], full details will only be given in a subsequent publication.

Both the optimal focusing conditions and the electron velocity energy scale calibration of the photoelectron imaging spectrometer were obtained from observations of Cu^- , whose electron affinity (1.236 eV) is well established [24]. With appropriate adjustment of the photoelectron imaging optics, the energy resolution (ΔE) of the photoelectron spectrometer is measured to be 19 meV at 1.13 eV electron kinetic energy (eKE), with this image filling the detector. The resolution scales approximately as the square root of the kinetic energy for a given image magnification, and $\Delta E/E$ remains near 0.02 for the maximum energy electrons seen with other magnifications. The narrowest peak observed to date arises from Cu^- photodetachment, ~ 2 meV FWHM at a photoelectron kinetic energy of 50 meV, with the image magnification set such that a 70 meV image fills the detector. Significantly higher photoelectron energy resolution (especially with s-wave photoelectrons) is possible using the collinear threshold imaging method developed by Neumark and coworkers [17], but physical constraints associated with this approach would preclude our planned time resolved studies.

3. Results and discussion

3.1. $Cu^-(H_2O)$

The 568 nm photoelectron velocity image and the corresponding reconstructed energy spectrum of

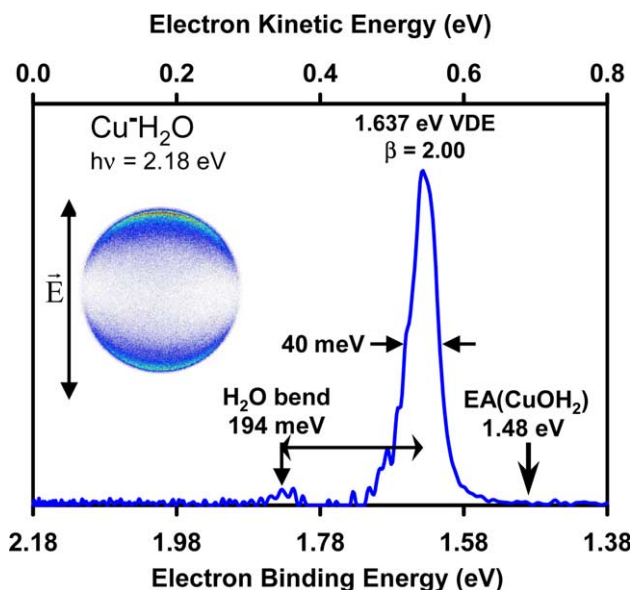


Fig. 2. Photoelectron image and spectrum of $\text{Cu}^-\text{H}_2\text{O}$ at 567.8 nm (2.184 eV). The intense peak corresponds to the vertical detachment energy near the neutral dissociation asymptote, not the 1.48 eV adiabatic electron affinity. See text for details.

$\text{Cu}^-\text{H}_2\text{O}$ are shown in Fig. 2. The magnification of the image was adjusted so as to fill the microchannel plate with 1 eV photoelectrons. Both eKE and the electron binding energy (eBE) are shown. The eBE is simply the photon energy less the eKE. The eKE is reported to illustrate the resolution for the peaks in the spectra as the wavelength is varied. The detachment wavelength is not only varied to access higher energy states, but to improve the resolution of a given feature by reducing the kinetic energy associated with it. The prominent peak in the spectrum is assigned as a transition producing the $[\text{Cu}^-(^2\text{S}), \text{H}_2\text{O}]$ state of the neutral complex. The vertical detachment energy (VDE) is measured to be 1.637(4) eV with $\beta = 2.00(1)$; Cu^- photodetachment provides the accurate reference value to calibrate the apparatus. The full-width half-maximum (FWHM) is 40 meV. A peak with intensity $\sim 10\%$ that of the intense ground state transition appears at 0.194 eV ($1570(20) \text{ cm}^{-1}$) higher binding energy with $\beta = 1.94(1)$ and is assigned as the H_2O bending mode. This energy separation is close to the ν_2 bending mode frequency of isolated H_2O , 1595 cm^{-1} [25]. Further experimental evidence supporting this assignment is provided by Margrave and coworkers [26] who co-condensed Cu atoms and H_2O in a cryogenic Ar matrix. They ascribed a 1573 cm^{-1} absorption band to the H_2O bend fundamental of the $\text{Cu}(\text{H}_2\text{O})$ complex.

The assignment of this peak to the ν_2 bending mode of H_2O was further confirmed by acquiring the photoelectron spectrum of $\text{Cu}^-(\text{D}_2\text{O})$. Though not shown in this Letter, the photoelectron spectrum of $\text{Cu}^-(\text{D}_2\text{O})$

exhibits a partially resolved feature located $1210(80) \text{ cm}^{-1}$ above the intense $[\text{Cu}^-(^2\text{S}), \text{D}_2\text{O}]$ transition. This energy difference is close to the 1178 cm^{-1} ν_2 bending frequency [25] of D_2O , adding further credence to assignment of the small peak in the $\text{Cu}^-(\text{H}_2\text{O})$ spectrum as arising from excitation of an essentially local water bending mode in the complex. The VDE of $\text{Cu}^-(\text{D}_2\text{O})$ is 1.638(4) eV, essentially the same as that of $\text{Cu}^-(\text{H}_2\text{O})$.

The appearance of this photoelectron spectrum is very similar to many others observed previously [27]. The presence of a single, intense, narrow feature with a short vibrational progression almost always reflects the photodetachment of a nonbonding electron and the production of a neutral molecule whose equilibrium geometry is essentially the same as the anion. The energy of the intense sharp peak should give an accurate measurement of the adiabatic electron affinity of the molecule. This ‘normal’ conclusion is incorrect for the copper–water system reported here.

The very long $\text{Cu}^--(\text{H}_2\text{O})$ bond length has the consequence that electron photodetachment produces a CuH_2O complex with a sufficiently large Cu–O separation that there are only weak $\text{Cu}^2\text{S}-\text{H}_2\text{O}$ interactions following photodetachment; calculations [2] indicate that the potential energy difference between the neutral photodetachment product (averaged over the anion vibrational wave function) and that of the separated Cu and H_2O components is $\sim 20 \text{ meV}$. This energy is approximately 80% of the 26 meV well depth indicated in Fig. 1. This result, coupled with the narrow line observed for this transition, gives a particularly simple method to obtain the anion dissociation energy through the cycle

$$D_0[\text{Cu}^--(\text{H}_2\text{O})] = \text{VDE}[\text{Cu}^-(\text{H}_2\text{O})] - \text{EA}[\text{Cu}] + \text{correction},$$

where $\text{EA}[\text{Cu}]$ is the electron affinity [24] of copper (1.236 eV), $\text{VDE}[\text{Cu}^-(\text{H}_2\text{O})]$ is the measured VDE, 1.637(4) eV, and the correction term is +20 meV, as obtained above. These quantities are depicted in Fig. 1. We thus find $D_0[\text{Cu}^--(\text{H}_2\text{O})]$ to be 0.42(2) eV. This result is in remarkably good agreement with that calculated by Taylor et al. [2], 0.44 eV.

The second consequence of this geometry difference is that the binding energy associated with the intense peak does not correspond to the adiabatic electron affinity, $\text{EA}(\text{CuH}_2\text{O})$. Rather, this quantity must be determined using the recent calculation [2] of the CuH_2O ground state surface to obtain the dissociation energy of the neutral complex, 0.16 eV. The adiabatic electron affinity is then given by the energy of the intense peak less this binding energy, with the result that $\text{EA}(\text{Cu}(\text{H}_2\text{O})) = 1.48(3) \text{ eV}$. The error estimate is largely based upon the uncertainties in the calculation of the neutral dissociation energy. Thus, the photoelectron spectrum,

even though exhibiting the single intense peak normally associated with the adiabatic electron affinity in fact has no detectable intensity at the electron energy corresponding to the actual adiabatic electron affinity, 1.48 eV. This energy is indicated by a vertical arrow in Fig. 2.

Photodetachment with 355 nm (3.49 eV) radiation accesses two excited electronic states [$\text{Cu } ^2\text{D}_{5/2, 3/2}, \text{H}_2\text{O}$] of the neutral complex. The two peaks corresponding to transitions to these states are quite broad (~ 140 meV) and appear at eBE of 3.050(15) and 3.313(15) eV, respectively. The additional width of these features (compared to the 40 meV width of the ground state transition) is an expected consequence of the greater size of $\text{Cu } ^2\text{D}$ compared to $\text{Cu } ^2\text{S}$. The β values for these two peaks are 0.16(3) and 0.19(3), respectively, consistent with electron detachment from an orbital different from the $\text{Cu}^- 4s$ orbital.

3.2. $\text{Cu}^-(\text{H}_2\text{O})_2$

The $\text{Cu}^-(\text{H}_2\text{O})_2$ ion is similar to $\text{Cu}^-(\text{H}_2\text{O})$, in the sense that the size difference between $\text{Cu}^- 3d^{10} 4s^{21}\text{S}$ and $\text{Cu } 3d^{10} 4s^2\text{S}$ ensures that electron photodetachment to produce the ground [$\text{Cu } (^2\text{S}), 2\text{H}_2\text{O}$] state again accesses portions of the neutral potential energy surface that have relatively weak interactions between the metal and the water molecules. If the two water molecules are located on opposite sides of Cu^- , then one would expect a peak with about twice the 40 meV width observed for $\text{Cu}^-\text{H}_2\text{O}$. If, however, the two water molecules are interacting as a ‘quasi hydrogen-bonded dimer’, then one expects significant changes in the water–water interaction upon electron detachment, and the ground state photoelectron spectrum peak would exhibit unresolved vibrational structure and more than twice the width observed for $\text{Cu}^-(\text{H}_2\text{O})$.

The 521 nm (2.379 eV) photoelectron spectrum of $\text{Cu}^-(\text{H}_2\text{O})_2$ is shown in Fig. 3. The VDE of the primary peak is 2.003(8) eV with $\beta = 1.86(2)$, and is ascribed to the [$\text{Cu } (^2\text{S}), 2\text{H}_2\text{O}$] state. This angular distribution is again very close to the $\cos^2(\theta)$ distribution expected for s-electron detachment, providing additional confirmation both of the state assignment and the physical model described above. The width of this peak is 100 meV; this width, more than twice that seen for CuH_2O , suggests that the two water molecules are interacting significantly, rather than being located on opposite sides of the metal. Recent calculations and dynamics studies [28] of $\text{Cu}^-(\text{H}_2\text{O})_2$ also support this conclusion.

A partially resolved peak appears $1540(80)\text{ cm}^{-1}$ above the origin and is again assigned to the ν_2 bending mode of H_2O . An additional 3.961 eV photoelectron spectrum of $\text{Cu}^-(\text{H}_2\text{O})_2$ (shown in Fig. 4) was acquired to detect the [$\text{Cu } ^2\text{D}_{5/2, 3/2}, 2\text{H}_2\text{O}$] states of

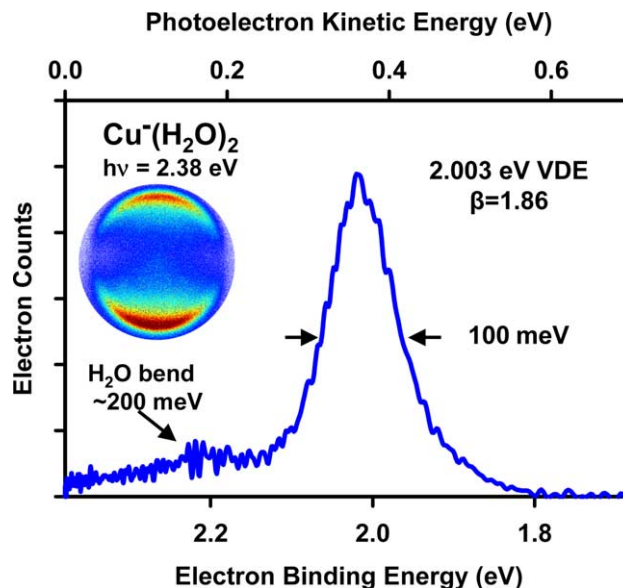


Fig. 3. Photoelectron image and spectrum of $\text{Cu}^-(\text{H}_2\text{O})_2$ at 521.2 nm (2.379 eV).

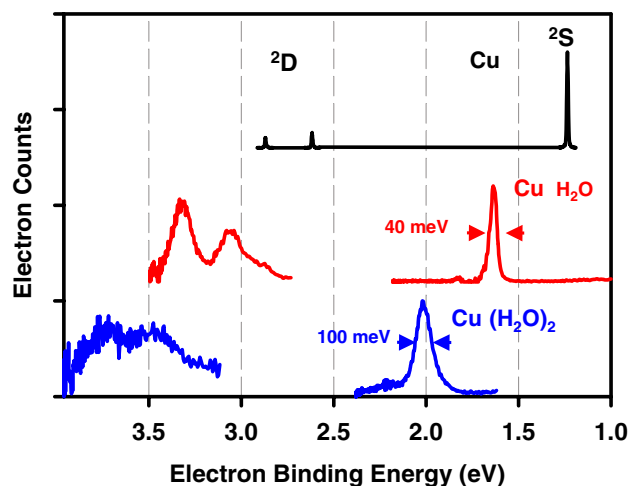


Fig. 4. Composite photoelectron spectra of $\text{Cu}^-(\text{H}_2\text{O})_n$ ($n=0,1,2$) showing the retention of the atomic level structure in the solvated complex, the progressive solvation broadening and the systematic solvation energy shift.

the complex. The [$\text{Cu } ^2\text{D}_{5/2}, 2\text{H}_2\text{O}$] component has a VDE of 3.50(7) eV with $\beta = 0.4(1)$, while the corresponding $^2\text{D}_{3/2}$ values are 3.72(7) eV and 0.3(1). As expected, the transitions to these states are even broader (250 meV) than the transition to the ground state of $\text{Cu}(\text{H}_2\text{O})_2$.

A composite view summarizing the photoelectron spectra of Cu^- , $\text{Cu}^-(\text{H}_2\text{O})$ and $\text{Cu}^-(\text{H}_2\text{O})_2$ is shown in Fig. 4. The solvation shifts and the systematic changes in line widths are clearly seen in this view. Equally clear is the conclusion that in all cases the excess charge remains largely localized on the metal

center, and that the low lying states are essentially perturbed atomic states.

4. Summary

A new photoelectron imaging spectrometer was employed to study the effects of solvation in the weakly-bound metal–ligand complexes $\text{Cu}^-(\text{H}_2\text{O})_n$ ($n = 1, 2$). The spectra demonstrate that the complexes are best characterized as a metal anion perturbed by H_2O adducts. The patterns of broadening in the spectra are readily understood in terms of the size relationships $R(\text{Cu}^- 3d^{10} 4s^2) \cong R(\text{Cu} 3d^9 4s^2) > R(\text{Cu} 3d^{10} 4s)$. While the excess charge is largely localized on the Cu atom, there is sufficient reduction of the H–O–H bond angle and charge delocalization onto the water adduct to excite the H_2O bending mode of CuH_2O upon electron photodetachment. The $\text{Cu}^-(\text{H}_2\text{O})$ photoelectron spectrum is highly atypical, in that the spectrum of the ground state exhibits an intense narrow peak and a short vibrational progression, normally indicative of very similar structure for the anion and neutral and implying that the binding energy of the intense peak is the adiabatic electron affinity. In this case, the substantial size difference between $\text{Cu}^- 3d^{10} 4s^2$ and $\text{Cu} 3d^{10} 4s$ results in no detectable intensity in the $\text{Cu}^-(\text{H}_2\text{O})$ photoelectron spectrum at the binding energy corresponding to the adiabatic electron affinity, and the energy of this transition instead relates to the anion dissociation energy.

Acknowledgements

We thank Prof. Andrei Sanov for numerous discussions and suggestions on the design of the imaging system. Dr. Vladimir Dribinski was extremely helpful on issues of data accumulation and analysis. We also thank Prof. Anne McCoy for theoretical work and discussions on the complexes. Finally, we acknowledge Mark Taylor and Jack Barbera for technical assistance on the pulsed discharge source. This work was supported by the National Science Foundation and the Air Force Office of Scientific Research.

References

- [1] F. Muntean, M.S. Taylor, A.B. McCoy, W.C. Lineberger, *J. Chem. Phys.* 121 (2004) 5676.
- [2] M.S. Taylor, F. Muntean, W.C. Lineberger, A.B. McCoy, *J. Chem. Phys.* 121 (2004) 5688.
- [3] A. Antusek, M. Urban, A.J. Sadlej, *J. Chem. Phys.* 119 (2003) 7247.
- [4] F. Misaizu, K. Tsukamoto, M. Sanekata, K. Fuke, *Surf. Rev. Lett.* 3 (1996) 405.
- [5] F. Misaizu, K. Tsukamoto, M. Sanekata, K. Fuke, *Laser Chem.* 15 (1995) 195.
- [6] D.W. Chandler, P.L. Houston, *J. Chem. Phys.* 87 (1987) 1445.
- [7] J.A. Davies, J.E. LeClaire, R.E. Continetti, C.C. Hayden, *J. Chem. Phys.* 111 (1999) 1.
- [8] L. Wang, H. Kohguchi, T. Suzuki, *Faraday Discuss.* 113 (1999) 37.
- [9] D. Conroy, V. Aristov, L. Feng, A. Sanov, H. Reisler, *Acc. Chem. Res.* 34 (2001) 625.
- [10] A. Eppink, D.H. Parker, *Rev. Sci. Instrum.* 68 (1997) 3477.
- [11] E. Surber, A. Sanov, *J. Chem. Phys.* 116 (2002) 5921.
- [12] E. Surber, R. Mabbs, A. Sanov, *J. Phys. Chem. A* 107 (2003) 8215.
- [13] R. Mabbs, E. Surber, A. Sanov, *Analyst* 128 (2003) 765.
- [14] R. Mabbs, K. Pichugin, E. Surber, A. Sanov, *J. Chem. Phys.* 121 (2004) 265.
- [15] A.V. Davis, R. Wester, A.E. Bragg, D.M. Neumark, *J. Chem. Phys.* 118 (2003) 999.
- [16] A.E. Bragg, J.R.R. Verlet, A. Kammrath, D.M. Neumark, *J. Chem. Phys.* 104 (2004) 3515.
- [17] A. Osterwalder, M.J. Nee, J. Zhou, D.M. Neumark, *J. Chem. Phys.* 121 (2004) 6317.
- [18] M.A. Johnson, W.C. Lineberger, in: J.M. Farrar, J.W. Saunders (Eds.), *Techniques for the Study of Ion Molecule Reactions*, Wiley, New York, 1988, p. 591.
- [19] J. Ho, K.M. Ervin, W.C. Lineberger, *J. Chem. Phys.* 93 (1990) 6987.
- [20] W.C. Wiley, I.H. McLaren, *Rev. Sci. Instrum.* 26 (1955) 1150.
- [21] M.E. Nadal, P.D. Kleiber, W.C. Lineberger, *J. Chem. Phys.* 105 (1996) 504.
- [22] A. Sanov, T. Sanford, S. Nandi, W.C. Lineberger, *J. Chem. Phys.* 111 (1999) 664.
- [23] V. Dribinski, A. Ossadtchi, V. Mandelshtam, H. Reisler, *Rev. Sci. Instrum.* 73 (2002) 2634.
- [24] R.C. Bilodeau, M. Scheer, H.K. Haugen, *J. Phys. B* 31 (1998) 3885.
- [25] T. Shimanouchi, *Tables of Molecular Vibrational Frequencies Consolidated Volume I*, National Bureau of Standards, Washington, DC, 1972.
- [26] J.W. Kauffman, R.H. Hauge, J.L. Margrave, *J. Phys. Chem.* 89 (1985) 3541.
- [27] K.M. Ervin, W.C. Lineberger, in: N.G. Adams, L.M. Babcock (Eds.), *Advances in Gas Phase Ion Chemistry*, JAI Press, Greenwich, 1992, p. 121.
- [28] M.S. Taylor, J. Barbera, C.P. Schulz, F. Muntean, A.B. McCoy, W.C. Lineberger, *J. Chem. Phys.* 122 (in press).